Bioorganic & Medicinal Chemistry 19 (2011) 6570–6575

Contents lists available at ScienceDirect

Bioorganic & Medicinal Chemistry

journal homepage: www.elsevier.com/locate/bmc

# Bendigoles D–F, bioactive sterols from the marine sponge-derived *Actinomadura* sp. SBMs009

Luke Simmons [a], Katrin Kaufmann [a], Ronald Garcia [a,b], Gertrud Schwär [b], Volker Huch [c], Rolf Müller [a,b,*]

[a] Department of Microbial Natural Products, Helmholtz Centre for Infectious Disease, Helmholtz Institute for Pharmaceutical Research Saarland (HIPS) and Saarland University, Saarbrücken 66123, Germany
[b] Department of Pharmaceutical Biotechnology, Saarland University, Saarbrücken 66123, Germany
[c] Department of Chemistry, Saarland University, Saarbrücken 66123, Germany

ARTICLE INFO

*Article history:*
Received 26 January 2011
Revised 21 April 2011
Accepted 23 May 2011
Available online 30 May 2011

*Keywords:*
Natural products
Marine actinomyces
Anti-inflammatory

ABSTRACT

Marine derived actinomycetes have become an important source of bioactive natural products. Here we report the structure and bioactivity of the bendigoles D–F (**1**–**3**), 3-keto sterols isolated from the new marine sponge derived bacterium, *Actinomadura* sp. SBMs009. The isolation of these compounds was guided by a novel high-content screen for NF-κB and glucocorticoid receptor (GR) activity, and cytotoxicity assays. The structures of **1**–**3** were determined by detailed analysis of NMR, MS, and single crystal X-ray diffraction data. Interestingly, **1** displayed cytotoxicity against the L929 (mouse fibroblast) cell line with an $IC_{50}$ approximated to 30 μM and was the most active inhibitor of GR-translocation, while **3** was the most effective inhibitor of NF-κB nuclear translocation with an $IC_{50}$ of 71 μM.



## 1. Introduction

Microbial natural products continue to provide both the raw materials and the design inspiration for the majority of pharmaceutical lead discovery and drug development.[1] However, after decades of fruitful bio-prospecting and drug discovery, the traditional sources of natural products (e.g., plants and terrestrial actinomycetes) are realizing the 'law of diminished returns'.[2] In the face of declining antibiotic and anticancer drug discovery rates, the marine environment has emerged as an important source of bioactive natural products. There are, for example, several exciting marine derived molecules currently on the pharmaceutical market, and dozens more progressing through the development pipeline.[3] In many cases the source organisms are as diverse as the molecular structures, yet bacteria living in close association with the larger 'host' organism, are often found to produce the metabolites of interest.[4] Marine sponges (Porifera) in particular harbor extremely rich and diverse populations of microorganisms, and have yielded many bioactive natural products.[4,5] Among the many small molecules reported from marine sponges, steroids are exceptionally abundant and diverse. By some estimates, marine sponge derived steroids display greater structural diversity than those reported from any other organism.[6] Here we report on our efforts to characterize bioactive secondary metabolites from newly isolated marine-derived actinobacteria. This work has yielded the bendigoles D–F (**1–3**), in addition to the previously described bendigole B (**4**). Compounds **1**–**4** were isolated based on their NF-κB inhibition and glucocorticoid receptor–protein binding properties observed in our newly developed high content screen for anti-inflammatory agents. In addition, we report a new strain of marine sponge-derived *Actinomadura*.

## 2. Results and discussion

### 2.1. New bioactive natural products

The *Actinomadura* sp. SBMs009 was isolated from tissue sections of the marine sponge *Suberites japonicus* using a technique developed for isolating marine bacteria.[7] A pellet of cell mass and XAD resin was separated from the culture broth by centrifugation and exhaustively extracted with ethyl acetate. The resultant organic oil was subjected to bioactivity guided fractionation utilizing newly developed NF-κB and glucocorticoid receptor (GR) translocation assays. This guided fractionation yielded the new sterols bendigoles D–F (**1**–**3**) and the previously reported bendigole B (**4**) as the active constituents. Bendigole D (**1**) was isolated as colorless prisms. A HREIMS ion at *m/z* 375.21668 ($[M]^+$) representing a molecular formula of $C_{22}H_{30}O_5$ was deduced and indicated 8 degrees of unsaturation in **1**. Inspection of the $^{13}C$ NMR data set allowed two of the four oxygen atoms to be assigned as carbonyl functionalities and the other two as alcohol groups based on the presence of two $sp^2$ carbons ($\delta_{C\text{-}3}$ 188.3, $\delta_{C\text{-}22}$ 180.8) and two $sp^3$ carbons ($\delta_{C\text{-}7}$ 70.4, $\delta_{C\text{-}12}$ 73.0), respectively. The presence

* Corresponding author.
*E-mail address:* rom@mx.uni-saarland.de (R. Müller).

0968-0896/$ - see front matter © 2011 Elsevier Ltd. All rights reserved.
doi:10.1016/j.bmc.2011.05.044

of the two hydroxyl groups was further supported by analysis of HREIMS fragmentation patterns which indicated the loss of one (−18.01106 amu) and two (−36.02114 amu) –OH groups, respectively. Further inspection of the $^{1}H$, $^{13}C$ NMR data (Table 1) indicated that **1** contained two methyl singlets ($\delta_{H\text{-}18}$ 0.86, $\delta_{H\text{-}19}$ 1.27), one methyl doublet ($\delta_{H\text{-}21}$ 1.26) and two oxygenated methines ($\delta_{H\text{-}7}$ 4.02, $\delta_{H\text{-}12}$ 3.95). The comparison of the $^{13}C$- and DEPT-edited HSQC data also indicated that bendigole D (**1**) contained two carbonyl resonances, two additional quaternary carbons, ten methines and four methylenes (Table 1). The spectroscopic data for **1** were similar to those reported for the bendigoles A and B (**4**), two related sterols previously isolated from the marine-derived actinomycete *Gordonia australis* Acta 2299.[8] The primary differences found between compounds **1** and **4** were in the HREIMS and $^{13}C$ NMR data sets. Comparison of the HRMS data revealed that **1** possesses an additional hydroxyl group, and inspection of the $^{1}H$ and $^{13}C$ NMR data supported this hypothesis, allowing the placement of an oxygen atom at position 7 ($\delta_{C\text{-}7}$ 70.4, $\delta_{H\text{-}7}$ 4.02). This is in contrast to both **4** and bendigole A, where a saturated methylene carbon resides at position 7 ($\delta_{C\text{-}7}$ 33.1, $\delta_{H\text{-}7}$ 1.85/0.94).[8] The relative (typical sterol) configuration of **1** was determined through an observed series of ROE cross-peaks (Fig. 2) from H-8, -15 and -17 to the axial methyl $H_3$-18, and from H-6β, -8 and H-11β to $H_3$-19.

Compound **2** displayed a HREIMS ion at *m/z* 373.23040 $[M+H]^+$ and was assigned a molecular formula of $C_{23}H_{32}O_4$. A detailed comparison of the $^{1}H$ and $^{13}C$ NMR spectra of **2** (data not shown) with those of **1** (Table 1) indicated that the core ABDC rings are the same. The side-chain of **2** was determined to have a methyl ketone attached to C-20 in contrast to **1**, which possesses the terminal carboxylic acid (Fig. 1). This assignment was supported by the single crystal X-ray diffraction structure obtained for **2** (Fig. 3; CCDC #801389).

Bendigole F (**3**) provided a HREIMS ion at *m/z* 403.24789 $[M]^+$, which corresponds to a chemical formula of $C_{24}H_{34}O_5$ and fits the recorded $^{13}C$ NMR spectroscopic data. Comparison of the 1D and 2D NMR data of **3** with that of **1** and **2** revealed that it too possesses the standard steroidal core ring system with –OH groups amending positions C-7 and C-12 and the ketone at C-3. The hexanoic acid side chain of **3** (Fig. 4) was determined by analysis of the COSY NMR data and supported by the single crystal X-ray diffraction data (Fig. 4; CCDC #801390).

Compound **4**, provided a HREIMS ion at *m/z* 357.24574 ($[M]^+$), which in combination with our observed NMR spectra matched the values previously reported in the literature for **4** and was confirmed by single crystal diffraction data.[8]

It should be noted that compounds **1** and **3** have been previously discussed in the literature as theoretical products of aerobic bile acid degradation in *Pseudomonas* sp. and from bile acid organic synthesis efforts.[9–11] To our knowledge however there are no previous reports on the isolation of the molecules nor of any report on the structures beyond speculated degradation pathways or synthetic products, respectively. Here we report the isolation, molecular structures and biological activity of these microbial metabolites for the first time.

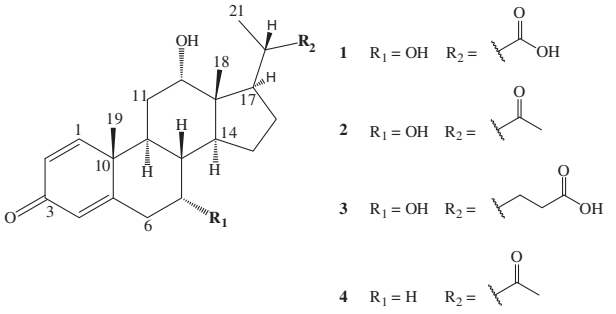


**Figure 1.** The molecular structures of compounds **1**–**4**.

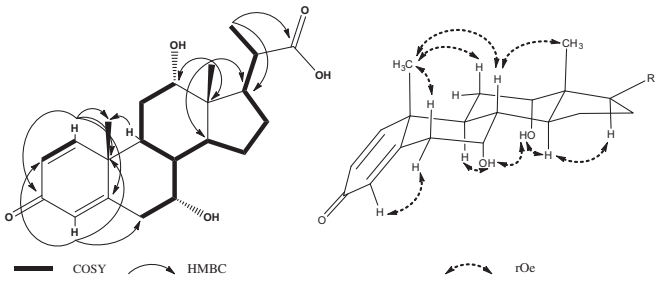


**Figure 2.** Selected 2D NMR correlations and cross-peaks for bendigole D (**1**).

**Table 1**
NMR spectroscopic data for compound **1** in $CD_3OD$; $^{13}C$ (125 MHz, $\delta_C$) and $^{1}H$ (500 MHz, $\delta_H$ (*J* in Hz))

| Position | $^{13}C$ | $^{1}H$ (multi, $J_{HH}$) | COSY[a] | HMBC[b] |
|---|---|---|---|---|
| 1 | 159.1 (CH) | 7.26 (d, 10) | 2 | 3,5,10,19 |
| 2 | 127.7 (CH) | 6.22 (d, 10) | 1 | 4,10 |
| 3 | 188.3 (C) | | | |
| 4 | 126.9 (CH) | 6.09 (s) | | 2,6,10 |
| 5 | 169.7 (C) | | | |
| 6 | 42.1 ($CH_2$) | 2.48/2.78 (m) | 7 | 4,5 |
| 7 | 70.4 (CH) | 4.02 (dd, 3) | 6, 8 | 5 |
| 8 | 39.8 (CH) | 2.00 (m) | 7,9,14 | 8,14 |
| 9 | 41.3 (CH) | 1.79 (m) | 8,11 | |
| 10 | 44.9 (C) | | | |
| 11 | 31.4 ($CH_2$) | 1.89/1.99 (m) | 9,12 | 13,18 |
| 12 | 73.0 (CH) | 3.95 (t, 2) | 11 | 9,14 |
| 13 | 47.7 (C) | | | 18 |
| 14 | 43.1 (CH) | 1.98 (m) | 8,15 | 18 |
| 15 | 27.7 ($CH_2$) | 1.39/1.80 (m) | 14, 16 | 14 |
| 16 | 24.3 ($CH_2$) | 1.27/1.79 (m) | 15, 17 | |
| 17 | 45.2 (CH) | 2.30 (m) | 16,20 | 21 |
| 18 | 13.1 ($CH_3$) | 0.86 (s) | | 12,13,14,17 |
| 19 | 18.7 ($CH_3$) | 1.27 (s) | | 8,10 |
| 20 | 43.9 (CH) | 2.35 (m) | 17,21 | |
| 21 | 16.8 ($CH_3$) | 1.26 (d, 7) | 17 | 17,20,22 |
| 22 | 180.8 (C) | | | |

[a] $^{1}H$–$^{1}H$ correlation spectroscopy.
[b] $^{1}H$–$^{13}C$ hetero-nuclear multiple bond correlation to the indicated position.

## 2.2. Bioactivity evaluation

NF-κB is a ubiquitous transcription factor in most eukaryotic cells. The NF-κB protein complex is a fast acting 'first responder' that is activated in response to inflammation, carcinogens, and other stimuli. Importantly, NF-κB has recently been shown to be constitutively activated in a variety of human cancer types.[12] In our efforts to screen microbial natural products for relevant pharmaceutical activity we developed an activity-based high-content screening (HCS) system for the quantification of NF-κB and glucocorticoid receptor (GR) translocation *in vivo*. We use the CHO cell line (hamster ovary) CHO/GFP-NF-κB from Affymetrix (Santa Clara, CA) stably expressing green-fluorescent protein (GFP)-coupled NF-κB. Treatment of the cells with the cytokine IL-1β induces translocation of the fluorescent protein from the cytoplasm into the nucleus. The GFP signal is then used for direct quantification of NF-κB translocation using Becton Dickinson's (BD) Pathway 855 High-Content Bioimager automated fluorescence microscope. Similarly, a system to quantify the movement of the glucocorticoid receptor (GR) signal transduction proteins was developed via the stable expression of a GR-EGFP fusion construct in U2OS, HaCaT and SH-SY5Y cell lines.[13]

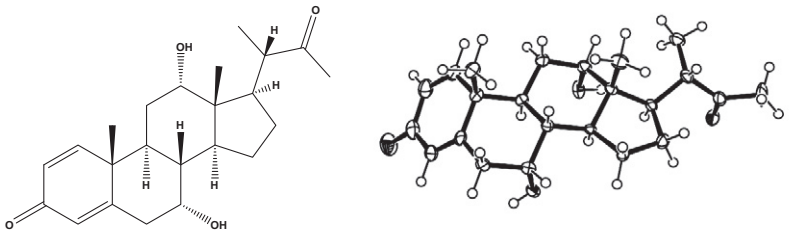

**Figure 3.** Structure and ORTEP rendering of bendigole E (**2**).

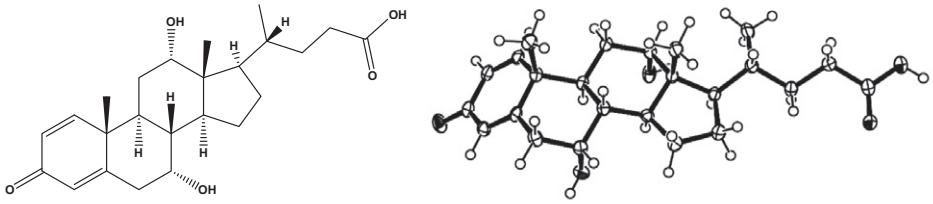

**Figure 4.** Structure and ORTEP rendering of bendigole F (**3**).

The organic fractions and pure compounds were screened against the NF-κB and GR assays, in addition to an MTT colorimetric assay to evaluate the compounds' cytotoxicity (Fig. 6). While each bendigole sterol displayed some anti-inflammatory activity, compound **3** proved to be the most active against the translocation of GFP-labeled NF-κB into the nucleus of the CHO cells with an $IC_{50}$ of 71 μM (Fig. 5a). Interestingly, our results indicate that compounds **1**–**3** displayed activity against the GR-translocation; in this case bendigole D (**1**) is the most potent (Fig. 5b). Experiments with the HaCaT and U2-OS cell lines displayed similar results as the SH-SY5Y cells, but displayed lower levels of GR-translocation.

### 2.2.1. MTT cytotoxicity assay

The MTT assays performed with the purified material indicate that the compounds **2** and **3** are clearly non toxic at the indicated concentrations against the L929 murine aneuploid fibrosarcoma cell line, which was used as a reference cell line. Bendigole D (**1**) however, displayed mild cytotoxicity against the L929 cell line, with an $IC_{50}$ of approximately 30 μM (Fig. 6). The observed toxicity of **1** is interesting because this compound is not shown to inhibit translocation of NF-κB or induce GR-transduction proteins (Fig. 5). While 3-keto steroidal hormones such as cortisone, hydrocortisone and dexamethasone are well known for their effects on inflammation pathways, our data provide additional insights to these important structure–activity relationships.

## 2.3. Morphological, fatty acid, 16S rDNA, and phylogenetic analysis of *Actinomadura* sp. SBMs009

Strain SBMs009 was identified as *Actinomadura* sp. belonging to *Thermomonosporaceae* in suborder *Streptoporangiineae*. The new isolate was aerobic, Gram-positive, and capable of producing aerial

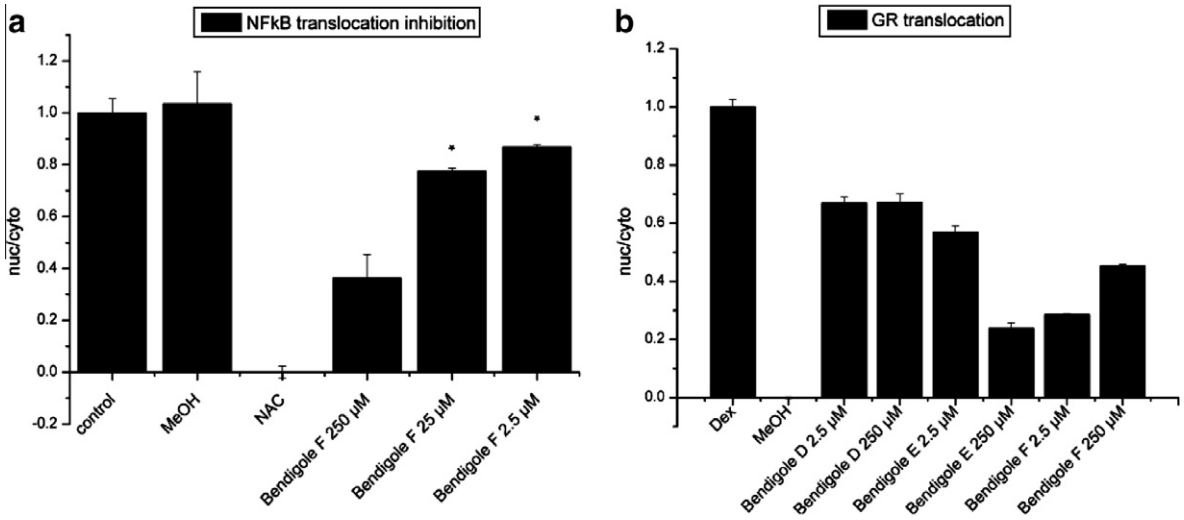


**Figure 5.** (a) Bar graph showing the inhibition of NF-κB translocation into the nucleus of CHO-NF-κB-GFP-cells treated with medium only (control) or 1% methanol (MeOH) or induced by bendigole F (**3**) (in 1% MeOH). The cell nuclei were stained with HOECHST and GFP-fluorescence was measured and quantified. The ratio of nuclear and cytoplasmic GFP-fluorescence was calculated (nuc/cyto), relative to *N*-acetyl-cysteine (NAC, 0) and MeOH, (1). ((x-min)/max–min)); (b) Bar graph showing the effects of **1**–**3** on GR-translocation in SH-SY5Y cells expressing GR-EGFP. Media containing 1% MeOH was used as the negative control and 100 nM dexamethasone as the positive control. Bars represent observed changes after incubation with 2.5 or 250 μM bendigole D (**1**), E (**2**) or F (**3**) for 1 h. The cell nuclei were stained with HOECHST to allow a segmentation of cytosol and nucleus and GFP-fluorescence in cytoplasm and nucleus. The ratio of nuclear and cytoplasmic GFP-fluorescence was calculated (nuc/cyto), relative to MeOH (0) and dexamethasone (Dex, 1). ((x-min)/max–min)). The experiments were carried out in duplicates. The asterisk marks those experiments that were accomplished twice in duplicates.

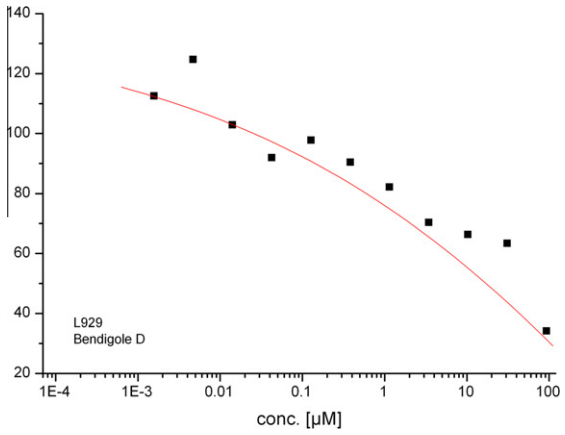


**Figure 6.** MTT assay results showing the non-linear dose–response curve of L-929 cells affected by **1**. *X*-axis displays cell growth as % of control; *Y*-axis shows concentration of **1** (μM).

and substrate non-fragmenting branched mycelia. Arthrospores are smooth oval to bean-shaped, measuring 1–2 μm in length, refractile and with a phase-dark coat. They appear as spirals or hooks of up to 15 spores. The strain produces a brown diffuse pigment around the colony which can be differentiated from non-pigmented *Actinomadura catellatispora*, and violet color produced by *Actinomadura livida*.[14] The latter soil dwelling actinomycetes are notable for its scanty aerial mycelia and uneven spore surface, whereas strain SBMs009 exhibits dense aerial mycelia and smooth spore surface-type. The difference from *A. catellatispora* was visually recognizable as a variation in spore chain-type.[13] The new bacterium is unusual for members of the genus *Actinomadura* in that it can grow and tolerate high salt concentration similar to that of the marine environment. However, this was not surprising since the strain was isolated from a marine sponge. Its significant amount of *iso*-C16:0 fatty acid (FA) (39.5%), C16:0 (12.2%) and C18:0 (8.5%) suggests a type 3a FA and thus supports SBMs009 FA chemo-taxonomy to genus *Actinomadura*.[15]

Based on 16S rDNA BLASTn alignments, SBMs009 is most similar to *A. livida* strains (98–99%), *A. hallensis* (96%), and other *Actinomadura* spp. (96–99%). Although highest identity was found with *A. livida*, the new isolate appears phylogenetically distant (Fig. 7). Their bifurcation was supported by 86.7% bootstrap values. Overall the unique differences in phenotypic, physiologic and phylogenetic characteristics are reflective of ecological adaption, and therefore suggest that SBMs009 represents a new species.

## 3. Experimental

### 3.1. General experimental procedures

All NMR spectra were measured on a Bruker Avance-500 instrument, using a 5 mm inverse-detection probe for $^{1}$H-, $^{1}$H–$^{1}$H COSY, $^{1}$H–$^{13}$C HMBC, $^{1}$H–$^{13}$C HSQC and $^{1}$H–$^{1}$H ROESY experiments, and 5 mm BBO probe for $^{13}$C experiments. High-accuracy mass spectra were measured using electrospray ionization with Thermo Scientific LTQ-Orbitrap Mass Spectrometer with nano-ESI inlet. Semi-preparative HPLC was performed using a Waters auto purifier LC–MS system running MassLynx software. Compound purification was performed using a Waters X-bridge C18 RPHPLC column.

### 3.2. Bacterial cultivation and fermentation

The strain *Actinomadura* sp. SBMs009 was cultivated and maintained on modified marine agar with 1.5–2% agar (MMA) and its liquid medium counterpart (MMB). The broth components are as follows (per 1000 mL): 5.0 g Peptone Casein (Difco), 1.0 g Yeast Extract (Difco), 20.0 g NaCl, Sea water salt solution 100 mL (from 10× stock solution), 900 mL $H_2O$, pH was adjusted to 7.5 with 1 M NaOH.[7] Shake flask fermentation (10 L) was performed in 5 L baffled flasks containing 2 L MMB medium, 10% 5-day inocula, and 2% sterile Amberlite resin XAD-16 (Sigma–Aldrich). Pre-culture inocula came from 1.0 $cm^2$ agar plugs cultivated for 5 days in 300 mL baffled flasks at 30 °C, @170 rpm. The same cultivation conditions were followed in 10 L fermentation, except for longer incubation (10 days).

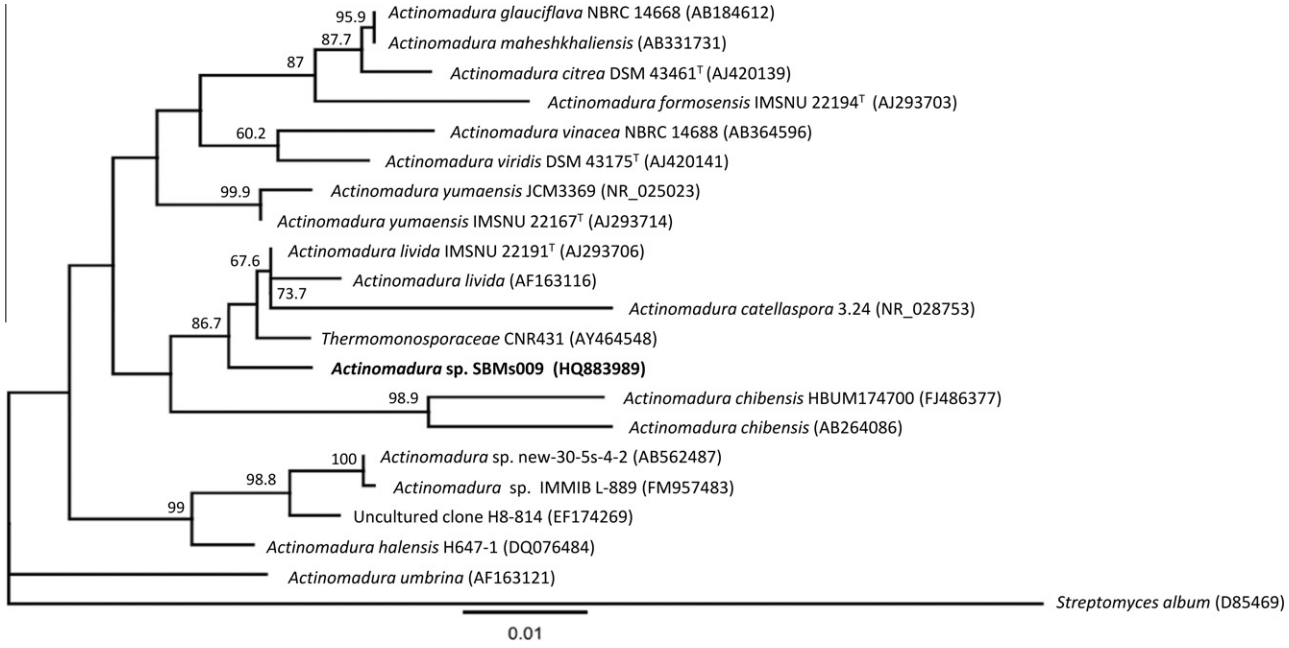


**Figure 7.** Phylogenetic tree of *Actinomadura* sp. SBMs009 based on 16S rRNA gene sequences; GenBank accession numbers are indicated in parenthesis. Only bootstrap values greater 60 were shown. Bar indicates the nucleotide substitutions per site.

### 3.3. Morphological observations and fatty acid analysis

Colony morphology was observed under dissecting and phase-contrast microscope taken from MM agar. Samples for fatty acid (FA) analysis were obtained from 1.0 mL actively growing culture in MMB medium (5 days), shaken at 160 rpm, 30 °C. FA extractions (in triplicate) were performed using the fatty acid methyl esters (FAME) method, and analyzed by GC–MS.[16]

### 3.4. 16S rDNA analysis and phylogenetic tree construction

Amplification and sequencing of 16S rDNA using universal primers were as previously described.[17] Complete 16S sequence of the strain was deposited in GenBank under accession number HQ883989. 16S DNA similarity with other microorganisms was performed by BLASTn 2.2.24+ search.[18] Other *Actinomadura* 16S rDNA sequences used in this study were obtained from GenBank with *Streptomyces album* (D85469) used as the out-group. Sequence alignments were performed using the rapid multiple sequence alignment based on fast Fourier transform (MAFFT) v.6.814b.[19] Distance matrices between sequences were calculated using Kimura.[20] The phylogenetic tree was constructed using the maximum likelihood method PHYML v2.4.5; a bootstrap of 1000 replicates was calculated.[21,22] Phylogenetic relationships were also confirmed using the Neighbor-joining and MrBayes version 3.1 methods.[23,24] These data were then complied using the Geneious Pro 5.0.2 software.[25]

### 3.5. Extraction and isolation

*Actinomadura* sp. SBMs009 mycelia and XAD resin were recovered from the culture media by centrifugation (10,000 rpm; 20 min) and extracted with ethyl acetate (EtOAc; 500 mL until clear) and filtered over Whatman paper. The EtOAc extracts were concentrated under reduced atmosphere, combined and washed with saturated NaCl. The resultant organic fraction was concentrated under vacuum and fractionated on a silica gel flash column. Fractions were eluted sequentially with [2:1] hexanes/EtOAc, [1:1] hexanes/EtOAc, [1:2] hexanes/EtOAc, 100% EtOAc, [2:1] EtOAc/MeOH, [1:1] EtOAc/MeOH, [1:2] EtOAc/MeOH, 100% MeOH. All fractions were submitted for bioactivity screening against our anti-inflammatory assay. The EtOAc fraction (56.3 mg) was shown to be active and was analyzed by RP18-HPLC/MS (Waters X-bridge 2.0 × 150 mm; $H_2O$/MeCN (+0.1% formic acid) [95:5] to [5:95] linear gradient). Compounds **1** (1.5 mg), **2** (1.0 mg), **3** (2.0 mg) and **4** (2.4 mg) were isolated using a Waters X-bridge semi-preparative column under the same conditions, and shown to induce the reported anti-inflammatory response.

### 3.6. X-ray single-crystal structure determination of 2 and 3

Crystals for structure determination were grown from MeCN in water. Thin prism shaped colorless crystals (approximately $0.04 \times 0.12 \times 0.41/0.06 \times 0.22 \times 0.23$ mm$^3$) were selected for data collection. The data sets were gathered at 153 K on an X8-Apex Bruker-AXS diffractometer (MoK$\alpha$ radiation). In the range from 2° to 27° $\theta$ collected reflections yielding in 3894/4598 independent reflections ($R_{int}$ = 0.06/0.03). We determined for **2** the orthorhombic space group $P2_12_12_1$ with a unit cell of $a$ = 7.7560(6), $b$ = 12.554(1), $c$ = 20.135(2) Å and for **3** the monoclinic space group $P2_1$ with $a$ = 6.0388(4), $b$ = 9.3762(6), $c$ = 20.075(1) Å, $b$ = 95.092(3)°. The structures were solved by direct methods,[26] showing the positions of all non hydrogen atoms. Subsequent refinement revealed the position of hydrogen atoms in Difference Fourier maps. Full-matrix least-squares refinement against $F_o^2$ with anisotropic thermal parameters (371/424 parameter) resulting in $R_1$ = 0.053/0.042 and $wR_2$ = 0.082/0.085 with $I > 2\sigma_I$. Further details are available from Cambridge Crystallographic Data Center under the depository numbers CCDC 801389 and 801390, respectively.

### 3.7. Bioactivity assays

#### 3.7.1. NF-κB anti-inflammatory assay

The cell line CHO-GFP-NF-κB was stimulated with 20 ng/mL IL-1β to induce translocation of NF-κB into the nucleus. To determine whether the IL-1β induced translocation of NF-κB could be retained cells were incubated for 4 h with the antioxidant NAC or dexamethasone as an alleviated translocation inhibitor. As shown in Figure 5a, NAC prevents IL-1β induced NF-κB translocation into the nucleus.

#### 3.7.2. GR anti-inflammatory assay

The cell lines U2OS, HaCaT and SH-SY5Y expressing GR-EGFP were stimulated with 100 nM dexamethasone for 1 h, the nuclei were stained with HOECHST to allow segmentation of cells with the BD AttoVision programme based on GFP-fluorescence in the nuclei and in the cytoplasm.

#### 3.7.3. MTT assay

Cells from different cell lines were seeded at a cell number of $10^3$ cells per well in a 96 well plate and after 24 h the substances were added and cell viability of cells was observed over 5 days. Then MTT solution (5 mg/mL in PBS) was added and the cells were incubated for an additional 4 h. Medium was aspirated and the formazan crystals generated by mitochondrial dehydrogenases of proliferating cells were dissolved in 10% SDS/0.01 M HCl. The absorption of the solution was measured at a wavelength of 570 nm.

#### 3.7.4. Cell lines used

U2OS, an osteosarcoma cell line is used as a reference cell line. These cells have adherent growth characteristics which are easy to monitor because of their planar growth, distinct cell shape and their relatively large size.[27] The cells are grown in McCoy's 5a media, 10% FCS. The following cell lines were also transduced for expression of GR-EGFP: (a) HaCaT, a human keratinocyte cell line grown in Dulbecco's Modified Eagles Medium (DMEM), 10% FCS; (b) SH-SY5Y, a human neuroblastoma cell line growing in DMEM, 15% FCS; and (c) L929 a mouse subcutaneous connective tissue fibroblast cell line growing in Roswell Park Memorial Institute (RPMI) 1640 medium, 10% FCS.

#### 3.7.5. Stable transfection of cell lines

We used the lentiviral transduction method to transfect mammalian cell lines with an expression vector encoding a fusion protein of the glucocorticoid receptor and EGFP.[28] The exact procedure for generation of the stable cell lines will be described in a subsequent paper. For testing the cells in translocator assays the cells are seeded into 96 well plates $5 \times 10^3$ cells per well. GFP-intensity in living cells is measured in the Pathway Bioimager 855.[13]

#### 3.7.6. Treatment of cells expressing GR-EGFP

Cells expressing GR-EGFP were seeded to $5 \times 10^3$ cells per well in a 96 well imaging plate (BD). The following day, the cells are treated with either 100 nM dexamethasone or different concentrations of the indicated substances for 1h. The cells were then stained with HOECHST. The resultant GFP signal intensity in the living cells was measured in the Pathway Bioimager. HOECHST staining is carried out by washing cells with PBS (phosphate buffered saline; 100 mM NaCl, 2.7 mM KCl, 10 mM $Na_2HPO_4$, 1.76 mM $KH_2PO_4$, pH 7.4), adding 4% paraformaldehyde in PBS for 10 min, washing with PBS incubating with HOECHST,

1 μg/mL, for 15 min in the dark, aspirating staining solution and adding PBS.

### 3.7.7. Treatment of CHO-NF-κB-p65-GFP cells

The CHO/GFP-NF-κB-p65 cell line was obtained from Affymetrix (part #RC2001). This cell line is designed for monitoring the activity of NF-κB transcription factor in cell-based assays. The CHO/GFP-NF-κB-p65 cell line was obtained by co-transfection of an expression vector for a fusion protein of GFP and human NFkBp65, as well as pHyg into Chinese hamster ovary (CHO) cells. Cells were then grown in the presence of hygromycin. These cells constitutively express the GFP-NF-κB-p65 fusion protein. Translocation of the GFP-NF-κB-p65 fusion protein from the cytoplasm to the nucleus can be visualized after stimulation with IL-1β. The functional assay was employed as described elsewhere.[13] Briefly, the cells were seeded at $10^5$ cells per well in a 96 well imaging plate (BD), left serum free for 4 h and simultaneously treated with 20 mM NAC or different concentrations of the indicated substances. The cells were then stimulated with 25 ng/mL IL-1β for 30 min and measured as described with the GR-GFP-expressing cells.

## Acknowledgments

This research was supported by the Deutsche Forschungsgemeinschaft and the Bundesministerium für Bildung und Forschung to R.M. and by the Alexander von Humboldt Foundation for the Research Fellowship to L.S. We would like to thank Dr. Junichi Tanaka for the *Suberites japonicas* specimen.

## Supplementary data

Supplementary data (1D and 2D NMR data for compound **1**) associated with this article can be found, in the online version, at doi:10.1016/j.bmc.2011.05.044.

## References and notes

1. Newman, D. J.; Cragg, G. *J. Nat. Prod.* **2007**, *70*, 461.
2. Fischbach, M. A.; Walsh, C. T. *Science* **2009**, *325*, 1089.
3. Mayer, A. M. S.; Glaser, K. B.; Cuevas, C.; Jacobs, R. S.; Kem, W.; Little, R. D.; McIntosh, J. M.; Newman, D. J.; Potts, B. C.; Shuster, D. E. *Trends Pharmacol. Sci.* **2010**, *31*, 255.
4. Simmons, T. L.; Coates, R. C.; Clark, B. R.; Engene, N.; Gonzales, D.; Esquenazi, E.; Dorrestein, P. C.; Gerwick, W. H. *Proc. Natl. Acad. Sci. U.S.A.* **2008**, *105*, 4587.
5. Blunt, J. W.; Copp, B. R.; Munro, M. H. G.; Northcote, P. T.; Princep, M. R. *Nat. Prod. Rep.* **2010**, *2*, 165.
6. Djerassi, C.; Silva, C. J. J. *Acc. Chem. Res.* **1991**, *24*, 371.
7. Iizuka, T.; Jojima, Y.; Fudou, R.; Yamanaka, S. *FEMS Microbiol. Lett.* **1998**, *169*, 317.
8. Schneider, K.; Graf, E.; Irran, E.; Nicholson, G.; Stainsby, F. M.; Goodfellow, M.; Bordon, S. A.; Keller, S.; Süssmuth, R. D.; Fiedler, H.-P. *J. Antibiot.* **2008**, *61*, 356.
9. Birkenmaier, A.; Holert, J.; Erdbrink, H.; Moeller, H. M.; Friemel, A.; Schoenenberger, R.; Suter, M. J.-F.; Klebensberger, J.; Philipp, B. *J. Bacteriol.* **2007**, *189*, 7165.
10. Iqbal, M. N.; Elliot, W. H. *Steroids* **1989**, *53*, 413.
11. Mukai, A.; Yazawa, K.; Katsukiyo, M.; Harada, K.; Graefe, U. *J. Antibiot.* **2005**, *58*, 356.
12. Pahl, H. L. *Oncogene* **1999**, *18*, 6853.
13. Kaufmann, K. et al., A paper providing a detailed description of the new HCS assays and their general applications for natural products discovery is currently in preparation.
14. Kroppenstedt, R. M.; Goodfellow, M. The Family *Thermomonosporaceae*: *Actinocorallia*, *Actinomadura*, *Spirillospora* and *Thermomonospora*. In *The Prokaryotes*; Dworkin, M., Falkow, S., Rosenberg, E., Schleifer, K.-H., Stackebrandt, E., Eds.; Springer: New York, 2006; pp 682–724.
15. Kroppenstedt, R. M. Fatty Acid and Menaquinone Analysis of Actinomycetes and Related Organisms. In *Bacterial Systematics*; Goodfellow, M., Minnikin, D. E., Eds.; Academic Press: London, 1985; pp 173–199.
16. Garcia, R.; Pistorius, D.; Stadler, M.; Müller, R. *J. Bacteriol.* **2011**, in review (01/2011).
17. Garcia, R.; Gerth, K.; Stadler, M.; Dogma, I. J.; Müller, R. *Mol. Phylogenet. Evol.* **2010**, *57*, 878.
18. Zhang, Z.; Schwartz, S.; Wagner, L.; Miller, W. *J. Comput. Biol.* **2000**, *7*, 203.
19. Katoh, M.; Kuma, M. *Nucleic Acids Res.* **2002**, *30*, 3059.
20. Kimura, M. *Proc. Natl. Acad. Sci. U.S.A.* **1981**, *78*, 454.
21. Guindon, S.; Gascuel, O. *Syst. Biol.* **2003**, *52*, 696.
22. Felsenstein, J. *Evolution* **1985**, *39*, 783.
23. Saitou, N.; Nei, M. *Mol. Biol. Evol.* **1987**, *4*, 406.
24. Huelsenbeck, J. P.; Ronquist, F. *Bioinformatics* **2001**, *17*, 754.
25. Drummond, A. J.; Ashton, B.; Buxton, S.; Cheung, M.; Heled, J.; Kearse, M.; Moir, R.; Stones-Havas, S.; Sturrock, S.; Thierer, T.; Wilson, A. Geneious Pro 5.0.2, 2010. Available from http://www.geneious.com.
26. Sheldrick, G. M. *Acta Crystallogr., Sect. A* **2008**, *64*, 112.
27. Gasparri, F.; Cappella, P.; Galvani, A. *J. Biomol. Screen.* **2006**, *11*, 586.
28. Lois, C.; Hong, E. J.; Pease, S.; Brown, E. J.; Baltimore, D. *Science* **2002**, *295*, 868.